Malaysian Journal of Chemistry, 2025, Vol. 27(3), 254-260
(Special Issue: *2nd International Science and Technology Colloquium, i-COSTECH 2024*)

Interlayer Expansion and Morphological Transformation of Zinc-Aluminium Anionic Clay through Methyl Orange Intercalation

Nursyafiqah Jori Roslan[1], Alsya Haneeza Mohd Shah[1], Nur Nadia Dzulkifli[1], Tengku Shafazila Tengku Saharuddin[2], Ruhaida Rusmin[1], Ainil Hawa Jasni[4], Hari Shankar Biswas[5], Vadym Kovalenko[6] and Sheikh Ahmad Izaddin Sheikh Mohd Ghazali[1]*

[1]Material, Inorganic and Oleochemistry (MaterInoleo) Research Group, School of Chemistry and Environment, Faculty of Applied Sciences, Universiti Teknologi MARA (UiTM), 72000 Kuala Pilah, Negeri Sembilan, Malaysia
[2]Industrial Chemical Technology Programme, Faculty of Science & Technology, Universiti Sains Islam Malaysia (USIM), 71800, Nilai, Negeri Sembilan, Malaysia
[3]Faculty of Applied Sciences, Universiti Teknologi MARA, 40450 Shah Alam, Selangor, Malaysia
[4]School of Medical and Life Sciences, Sunway University, 47500 Petaling Jaya, Selangor, Malaysia
[5]Department of Chemistry, Surrendranath College, 24/2, M.G. Road, Kolkata-09, India
[6]Department of Analytical Chemistry and Chemical technologies o food Additives and Cosmetics, Faculty of Chemical Technologies and Ecology, Ukrainian State University of Chemical Technology, Dnipro 749005, Ukraine
*Corresponding author (e-mail: sheikhahmadizaddin@uitm.edu.my)

This study reports the Zinc-Aluminium layered double hydroxide compound (ZAL) intercalated with organic anions of methyl orange (ZAMO) dye via the co-precipitate method. The intercalation of ZAL with Methyl Orange (MO) was carried out under optimal conditions with a concentration of 0.2 M methyl orange, a pH of 7.5 ± 0.2 and an ageing time of 18 hours. The ZAL and ZAMO were characterised using Powder X-ray diffraction (PXRD), Attenuated Total Reflectance – Fourier Transform Infrared Spectroscopy (ATR-FTIR) and Field Emission Scanning Electron Microscopy (FESEM) to confirm the intercalation of the guest ion. The overall PXRD pattern of ZAL and ZAMO shows an expansion of the basal spacing from 8.7 Å to 24.7 Å, indicating excellent intercalation of the ZAL compound with MO. The FTIR spectrum of ZAL and ZAMO shows two significant bands at 3383 cm^{-1} and 3418 cm^{-1} attributed to the water molecules and water in the interlayer lattice respectively, and band peaks at 1170 cm^{-1} corresponding to the sulfonic acid of MO, confirming the presence of MO in ZAMO. The spatial orientation of ZAMO expresses the interlayer region value for the ZAL nanocomposites of 17.1 Å. The FESEM revealed the morphology of ZAL with an irregular, agglomerated, dense and non-porous plate-like structure after the ZAL was intercalated with MO and the structure exhibited an agglomerate with porous and irregular size and shape. These findings demonstrate the effective intercalation of MO into the ZAL framework, resulting in a nanocomposite with modified structural and morphological properties.

Keywords: Dye; hydrotalcite; intercalation; zinc-aluminium layered double hydroxide; co-precipitate method

Received: September 2024; Accepted: December 2024

Layered double hydroxides (LDHs), often referred to as anionic clays, are a class of materials that possess a unique structure composed of positively charged layers intercalated with anions. These materials have garnered significant interest due to their versatile applications in areas such as catalysis, environmental remediation, and drug delivery. The general formula for LDHs is $[(M^{II})_{1-\chi}(M^{III})_{\chi}(OH)_2]^{\chi+}(A^{m-}_{\chi/m}).nH_2O]$, where M^{II} and M^{III} are divalent and trivalent metal cations, respectively, and A^{n-} is an interlayer anion [1]. Zinc-aluminum layered double hydroxide (ZAL) is one of the most widely studied LDH systems due to its high chemical stability, ease of synthesis, and tunable properties. The ZAL structure consists of brucite-like layers where zinc and aluminum cations occupy octahedral sites, with hydroxide ions providing charge balance. The layers are positively charged due to the partial substitution of Zn^{2+} by Al^{3+} and the charge is neutralized by intercalating anions in the interlayer spaces [2-4].

MO is characterized by the presence of a central azo group (-N=N-) connecting two aromatic rings (**Figure 1**).

This azo dye is a widely used anionic azo dye, poses significant environmental risks due

†Paper presented at the 2nd International Science and Technology Colloquium (i-COSTECH 2024)

to its toxicity to aquatic life, persistence in the environment, and tendency to bioaccumulate in the food chain, potentially impacting human health through contaminated food sources [5-8]. Additionally, MO's vibrant color can negatively affect the aesthetics of water bodies, rendering them unsuitable for recreational use [9]. The removal of methyl orange and other anionic azo dyes (congo red, acid red 88, direct blue 71 etc.) from industrial wastewater is a crucial environmental challenge.

The unique layered structure of ZAL makes them highly promising candidates for the removal of pollutants like methyl orange from wastewater. ZAL have demonstrated exceptional adsorption capacity and selectivity for anionic dyes due to their positively charged layers and ability to intercalate guest anions between the layers. Intercalating MO into ZAL presents a promising strategy for removing and recovering this persistent dye from contaminated water, mitigating its ecological impact and contributing to environmental remediation efforts [10]. This process not only removes the dye but also stabilizes it, preventing its further release into the environment. This study aims to investigate the intercalation of methyl orange into the interlayer space of Zn-Al layered double hydroxides via ion exchange method and study the characteristic of the resulting material.

EXPERIMENTAL

Chemicals and Materials

All chemicals used in this study were of analytical grade $Zn(NO_3)_2.6H_2O$ hexahydrate, $Al(NO_3)_3.9H_2O$ nanohydrate and HCl were purchased from R&M Chemicals. Methyl Orange was purchased from Bendosen. NaOH was purchased from Merck (Germany). All reagents used were prepared with deionised water (DI) without further purification.

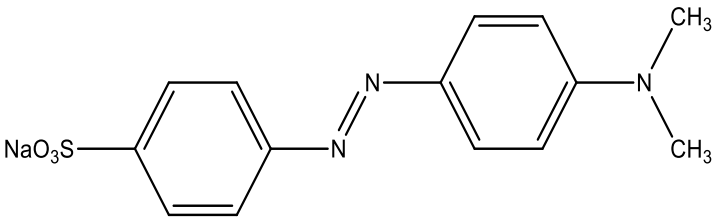

Figure 1. Chemical Structure of MO.

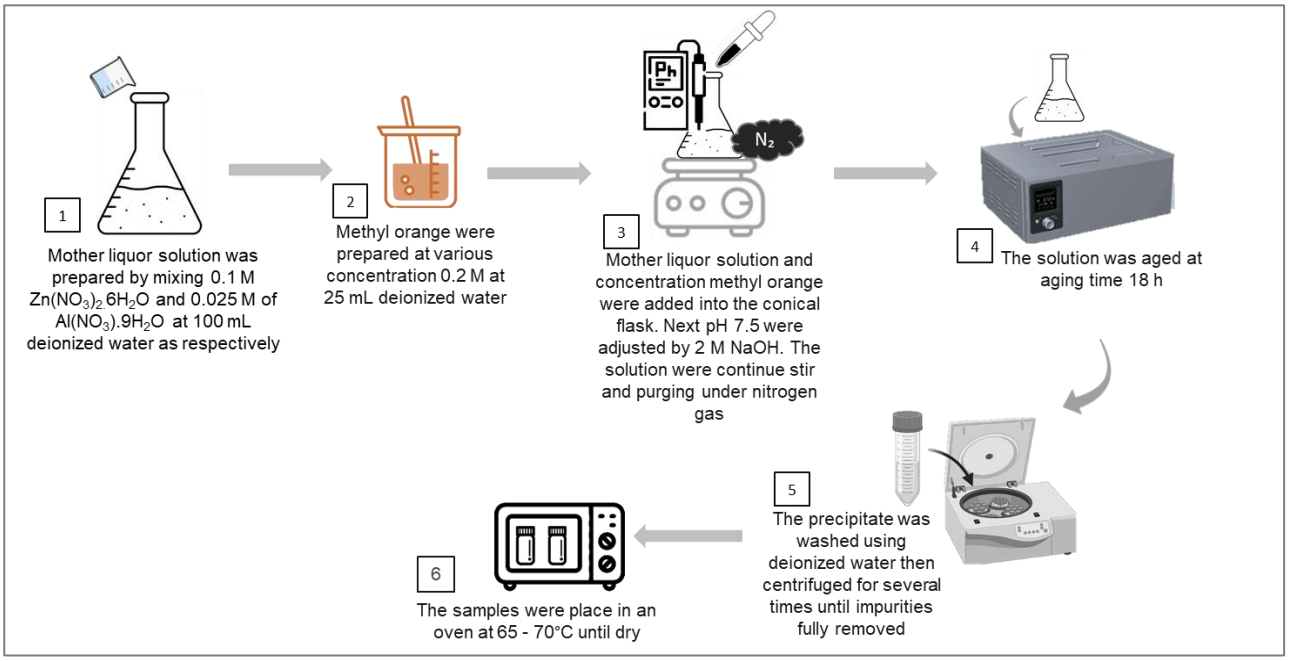

Figure 2. Schematic diagram of intercalation process of methyl orange with ZnAl-LDH nanocomposites.

Preparation of Intercalation Methyl Orange with ZnAl-LDH Nanocomposites using Co-precipitate Method

The synthesis of MO intercalation with Zinc-Aluminium-Layered double hydroxide (Zn-Al LDH) was performed according to procedures modified from [11] as illustrated in **Figure 2**. First, 0.1 M $Zn(NO_3)_2.6H_2O$ and 0.025 M $Al(NO_3)_3.9H_2O$ were respectively dissolved in a 100 mL deionized water. Meanwhile a 0.2 M methyl orange was prepared by dissolving a calculated amount of solid dye with 25 mL of deionized water. Then the solution was added to the mother liquor. Thirdly, a base solution was obtained by dissolving 2 M sodium hydroxide in 100 mL deionized water. Fourthly, the pH of the above mixture was adjusted to pH 7.5 ± 0.2 under vigorous stirring. The solution was aged 18 h in oil bath shaker at 70°C, until the orange precipitate was formed. The obtained orange precipitate was washed thoroughly using deionized water and then centrifuged several times until impurities were fully discarded. Finally, the orange slurry samples were dried in an oven at 65 - 70°C for 72 hours and ground for further characterization. It is worth mentioning that the intercalation process was carried out under air atmosphere.

Characterization and Spatial Orientation Modelling

A Bruker D8 Advance XRD diffractometer was used to record a PXRD pattern of the nanocomposite in the 2θ range between 5° and 70°, using CuKα radiation at 40 mA and 40 kV (λ = 1.54059 Å). The infrared spectra of ZAL, ZAMO and pure MO were obtained using an FTIR spectra 2000 spectrophotometer (Perkin Elmer) equipped with a diamond attenuated total reflectance (ATR) accessory. The spectra were recorded in the range of 4,000-400 cm^{-1} with a spectral resolution of 4 cm^{-1}.

The surface morphology of the materials was observed using FESEM using Supra 55VP. The ZAMO spatial orientation modelling was interpreted using software ChemDraw 3D Pro Software.

RESULTS AND DISCUSSION

Powder X-ray Diffraction (PXRD)

Figure 3 displays the PXRD patterns for the ZAL host, pure MO, and the intercalated nanocomposite at MO concentration of 0.2 M. Pure MO exhibits a broad peak in the range of 20°–30°=2θ, indicative of its amorphous nature and disordered molecular stacking. This broad peak makes assigning specific crystal planes difficult. The ZAL host, on the other hand, displays sharp reflections, characteristic of a well-ordered layered structure. Prominent peaks are observed around 10.30° and 22°=2θ. The XRD pattern of pristine ZAL (LDH-NO_3) exhibits strong basal reflections and at approximately 10° and 20°=2θ, respectively, corresponding to intercalated nitrate ions. Additionally, the presence of reflections between 30° and 37° = 2θ can be attributed to carbonate contamination, likely arising from atmospheric CO_3^{2-} during sample preparation. These reflections correspond to the (012), (104) and (015) crystalline planes of the LDH structure. The obtained ZAL is similar to the typical features of LDH with the basal spacing of 8.7 Å, which corresponds to the nitrate peaks as the counter anion [12]. In-plane reflections, such as and at ~60° and ~65°= 2θ, respectively, confirm the hexagonal arrangement of metal cations within the layers.

Upon intercalation of MO, the basal reflection shifts to a lower angle (around 3.5°= 2θ), indicating an expansion of the basal spacing from 8.7 Å to 24.7 Å. This significant increase confirms the successful incorporation of MO anions within the interlayer galleries of the ZAL host. The broadening of this peak in ZAMO suggests some variation in the interlayer spacing or a decrease in the stacking order. The XRD pattern of LDH-MO shows a shifted basal reflection at ~4°= 2θ (003), corresponding to an expanded interlayer distance due to the intercalation of MO molecules. Higher-order basal reflections (006) and in-plane reflections ((110), (200)) confirm that the intercalation primarily affects the interlayer structure while preserving the hexagonal arrangement within the layers. The observed changes in the diffraction pattern, including peak shifts and broadening, suggest a polymorphic transformation associated with the displacement of nitrate ions by the larger MO anions [13].

Attenuated Total Reflectance – Fourier Transform Infrared Spectroscopy (ATR-FTIR)

The ATR-FTIR spectra of ZAL host and ZAMO were shown in **Figure 4**. Based on the broad absorption peak in the ZAL host 3383 cm^{-1}, the peak is denoted by the stretching vibrations of the O-H function group caused by the adsorbed interlayer water of the hydroxyl of the layered structure. Other than that, the small peak at 1651 cm^{-1} belongs to the formation of bending water molecules, followed by the peak of nitrate, which occupies the counter anion at 1351 cm^{-1} [14]. The ZAMO nanocomposites exhibit broad brand centred at 3418 cm^{-1}, which corresponded to the O-H stretching vibration of water molecules in the interlamellar region as well as the bending of water molecules at 1607 cm^{-1}. Further, the significant peak of the nanocomposites is the newly formed peak at 1170 cm^{-1} attributed to sulfonic structure, -S=O stretching vibrations [15]. After the absorption band has slightly shifted from the original position due to the interaction process of the MO anion and the positively charged surface layers. According to the spectra of pure MO anion, the band at 1110 cm^{-1} have appeared for the nanocomposites ZAMO. This is due to the substitution of sulfonic acid to prove that the intercalation of MO is in the anionic form [16].

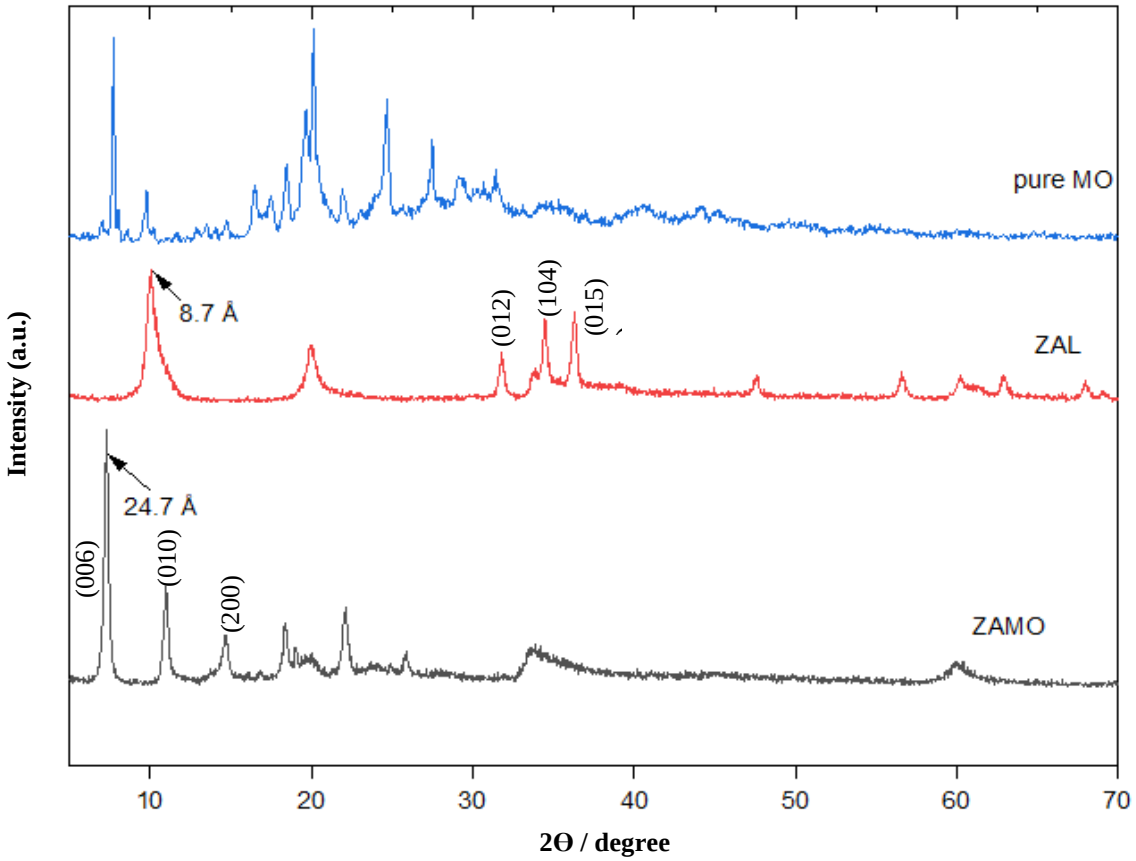

Figure 3. PXRD pattern of ZAMO nanocomposite, ZAL host and pure MO.

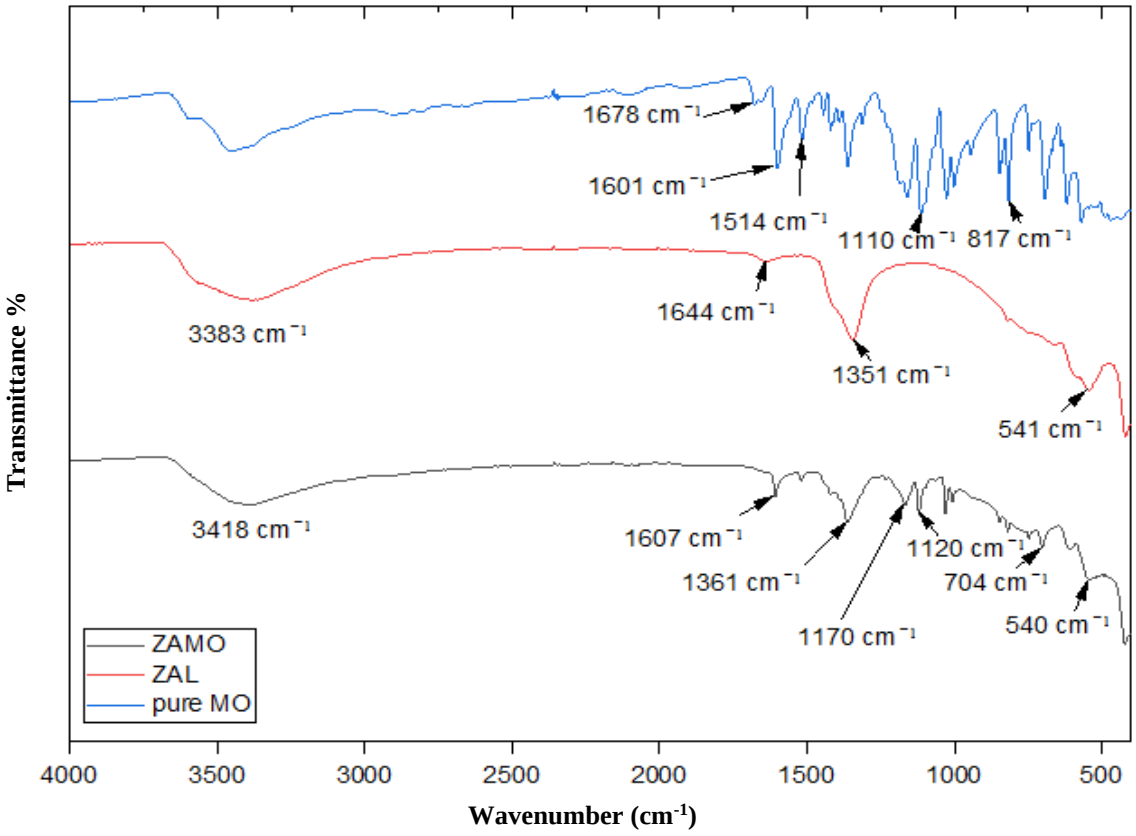

Figure 4. ATR-FTIR spectra of ZAMO, ZAL host and pure MO.

Table 1. Peaks observed in IR spectra for host and its nanocomposites.

Functional Group	Observed peaks (wavenumber cm^{-1})		
	ZAMO	ZAL	pure MO
O-H stretching	3383	3418	-
O-H bending	1607	1644	-
NO_3^- anion	1361	1351	-
S=O stretching vibration	1170	-	1110

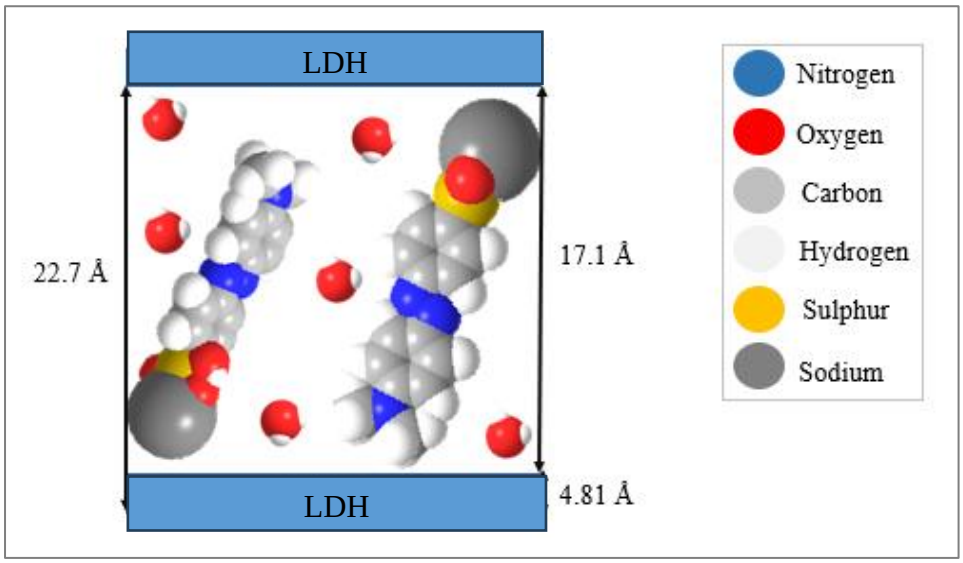

Figure 5: Molecular structural models of interaction ZAMO between the ZAL interlayers.

Table 1 summarizes the FTIR peaks for ZAMO, ZAL, and pure MO, highlighting the characteristic functional groups and their respective wavenumber regions. Therefore, from the FTIR analysis, the nanocomposites is consistent with the PXRD pattern, which supported the intercalation process of MO into the interlayer region of ZAL.

Spatial Orientation

The three-dimension molecular size of the MO anion and its theoretical spatial orientation arrangement are illustrated in **Figure 5**. As refer to the PXRD analysis above, the basal spacing for ZAL intercalated is 24.7 Å. Since the theoretical thickness LDH is 4.81 Å [17], the interlayer region of ZAMO can be calculated by subtracting the total basal spacing of the nanocomposite (24.7 Å as shown in **Figure 5**) giving its value of 17.1 Å. This value is the area allocated for the spatial orientation of MO anion as they displaced into the intergalleries of ZAL. Theoretically, the orientation of MO anions was likely to orientate in a vertical manner adjacent to the positively charged brucite layer ZAL and also due to the fields of benzene-benzene aromatic ring mutually by π-π interactions Hence, the value obtained for the interlayer ZAL is consistent to the enlargement of the ZAL after MO anion has intercalated into the layered structure.

Field Emission Scanning Electron Microscopy Spectroscopy (FESEM)

The surface morphology of ZAL and ZAMO nanocomposites was observed under 10,000x magnification as shown in **Figure 6**. ZAL morphology exhibited typical morphology of layered material, which is aggregated hexagonal plate-like with non-uniform particles of different sizes and shapes [18]. After the MO anion had intercalated into the interlayer region of ZAL, the structure formed into small shape of aggregated plate-like with higher surface area. This confirms the enlargement of basal spacing in the PXRD analysis in **Figure 3**.

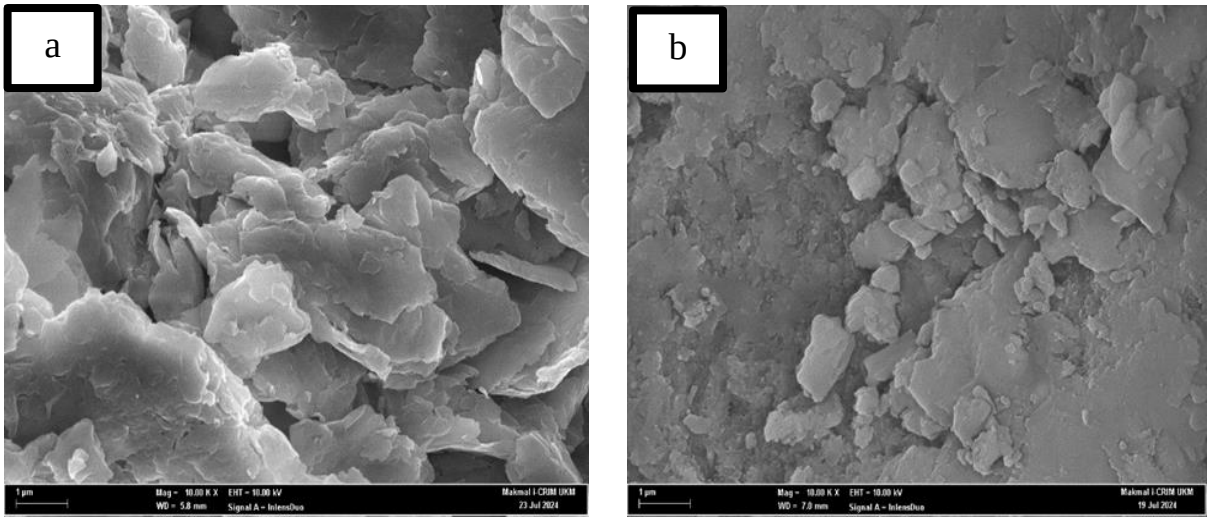

Figure 6: FESEM of (a) ZAL and (b) ZAMO at 10K magnification.

CONCLUSION

This study explores the intercalation of methyl orange dye into a Zn-Al layered double hydroxide compound via the co-precipitation method. The results from PXRD, ATR-FTIR, and FESEM analyses confirm the successful incorporation of the guest ion within the ZAMO nanocomposite. From the PXRD results, the expansion of basal spacing from 8.7 Å to 24.7 Å were observed and indicates the success of intercalation between ZAL and MO. The ATR-FTIR data provides further evidence of the characteristic functional groups associated with methyl orange, indicating its effective integration within the layered double hydroxide host. The FESEM data provides insights into the morphology and surface features of the ZAMO material. The expanded interlayer distance suggests the effective loading of methyl orange within the host layered double hydroxide structure, and from the data also reveals the polymorphic transformation during the intercalation process.

ACKNOWLEDGEMENTS

This research was funded by the Ministry of Higher Education (MOHE) under the Fundamental Research Grant Scheme (Grant number: FRGS/1/2023/STG05/ UITM/02/20)

REFERENCES

1. Bakhtaoui, N., Benali, O., Mazarío, E., Recio, F. J. & Herrasti, P. (2021) Layered double hydroxides intercalated with methyl orange as a controlled-release corrosion inhibitor for iron in chloride media. *Nano Express*, **2(1)**, 010017.

2. Ahmed, M. A. and Mohamed, A. A. (2023) A systematic review of layered double hydroxide-based materials for environmental remediation of heavy metals and dye pollutants. *Inorganic Chemistry Communications*, **148,** 110325.

3. Jiang, Y., Shen, Z., Tang, C. S. and Shi, B. (2023) Synthesis and application of waste-based layered double hydroxide: A review. *Science of the Total Environment*, **903**, 166245.

4. Sandollah, N. A. S. M., Ghazali, S. A. I. S. M., Wan Ibrahim, W. N., Rusmin R. (2020) Adsorption-desorption profile of methylene blue dye on raw and acid activated kaolinite. *Indonesian Journal of Chemistry*, **20 (4)**, 755–765.

5. A'srai, A. I. M., Razali, M. H., Amin, K. A. M. and Osman, U. M. (2023) CuO/TiO_2 nanocomposite photocatalyst for efficient MO degradation. *Digest Journal of Nanomaterials and Biostructures*, **3(18)**, 1005–1124.

6. Halim, N. H. M. H. and Razali, M. H. (2019) Methyl Orange Degradation using TiO_2 Powder and Immobilized TiO_2 Photocatalysts. *Universiti Malaysia Terengganu Journal of Undergraduate Research*, **4(1)**, 61–66.

7. Salleh, N. M., Mohsin, S. M. N., Sarijo, S. H., Ghazali, S. A. I. S. M. (2017) Synthesis and Physico-Chemical Properties of Zinc Layered Hydroxide-4-Chloro-2-Methylphenoxy Acetic Acid (ZMCPA) *Nanocomposite IOP Conference Series: Materials Science and Engineering*, **204 (1)**, 012012.

8. Kang, J., Xue, S., Cheng, C., Qin, J., Li, H., Li, A. J., Guo, W., Yin, R. and Qiu, R. (2024) Enhanced peroxydisulfate activation by photo-piezocatalysis

based on zinc-aluminum layered double hydroxide for imidacloprid removal: Combined radical with nonradical pathways. *Separation and Purification Technology*, **345**, 127341.

9. Li, T., Ma, Y., Liu, J. K., Liu, J. C., Liu, Z. X., Ma, Y. S. and Liu, P. P. (2024) In-situ construction of lamellar stacked zinc molybdate-zinc/aluminium layered double hydroxides heterojunction material with synergistic corrosion protection. *Progress in Organic Coatings*, **189**, 108294.

10. Barkhordari, S. and Alizadeh, A. (2024) Zinc/ aluminium-layered double hydroxide-gallic acid doped carboxymethyl cellulose nanocomposite films for wound healing. *International Journal of Biological Macromolecules*, **260**, 129556.

11. Li, K., Li, W., Zhao, Y., Liu, W., Tian, R. and Lin, Y. (2024) Highly atom-economic synthesis and scale-up production of zinc-aluminum layered double hydroxides. *Chemical Engineering Science*, **283**, 119376.

12. Gupta, N. K., Leyva, C., Viltres, H., Dhavale, R. P., Kim, K. S., Romero-Galarza, A. and Park, H. H. (2023) Zinc-aluminum layered double hydroxide and double oxide for room-temperature oxidation of sulfur dioxide gas. *Chemosphere*, **338**, 139503.

13. Abd Ghani, K. D., Nayan, S., Ghazali, S. A. I. S. M., Shafie, L. A. and Nayan, S. (2010) Critical internal and external factors that affect firms strategic planning. *International Research Journal of Finance and Economics*, **51**, 50–58.

14. Sharif, S. N. M., Hashim, N., Isa, I. M., Bakar, S. A., Saidin, M. I., Ahmad, M. S., Mamat, M. and Hussein, M. Z. (2020) The influence of chitosan coating on the controlled release behaviour of zinc/aluminium-layered double hydroxide-quinclorac composite. *Materials Chemistry and Physics*, **251**, 123076.

15. Cyril, N., George, J. B., Joseph, L. & Sylas, V. P. (2019) Catalytic Degradation of Methyl Orange and Selective Sensing of Mercury Ion in Aqueous Solutions Using Green Synthesized Silver Nanoparticles from the Seeds of Derris trifoliata. *Journal of Cluster Science*, **30(2)**, 459–468.

16. Fatimah, I., Citradewi, P. W., Yahya, A., Nugroho, B. H., Hidayat, H., Purwiandono G., Sagadevan, S., Ghazali, S. A. I. S. M. and Ibrahim, S. (2021) Biosynthesized gold nanoparticles-doped hydroxyapatite as antibacterial and antioxidant nanocomposite. *Materials Research Express*, **11(8)**, 115003.

17. Bohari, F. L., Izaddin, S. M. G. S. A., Dzulkifli, N. N., Baharin, S. N. A., Fatimah, I. and Poddar, S. (2023) Studies on the intercalation of calcium-aluminium layered double hydroxide-MCPA and its controlled release mechanism as a potential green herbicide. *Open Chemistry*, **21(1)**, 1–8.

18. Barahuie, F., Hussein. M. Z., Gani, S. A., Fakurazi, S. and Zainal, Z. (2015) Synthesis of Photocatechuic acid-zinc/aluminium-layered double hydroxide nanocomposite as an anticancer nano-delivery system. *Journal of Solid State Chemistry*, **221**, 21–31.